ELSEVIER

Catalysis Today 53 (1999) 607–612

CATALYSIS TODAY

www.elsevier.com/locate/cattod

Cerium–terbium mixed oxides as alternative components for three-way catalysts: a comparative study of Pt/CeTbO$_x$ and Pt/CeO$_2$ model systems

S. Bernal, G. Blanco, M.A. Cauqui *, M.P. Corchado, C. Larese,
J.M. Pintado, J.M. Rodríguez-Izquierdo

Departamento de Ciencia de los Materiales e Ingeniería Metalúrgica y Química Inorgánica,
Universidad de Cádiz. Apdo.40.11510 Puerto Real, Spain

Abstract

By using a combination of oxygen buffering capacity (OBC) and oxygen storage capacity (OSC) measurements, the redox behaviour of a Pt/CeTbO$_x$ catalyst is compared to that of a classic model TWC system: Pt/CeO$_2$. The results reported here show that the redox efficiency of the Pt/CeTbO$_x$ catalyst is much better, especially at low temperature operation conditions such as those occurring during the cold start of engines. The catalyst containing terbium also shows lower ‘light-off’ temperatures for both methane and carbon monoxide oxidation. ©1999 Elsevier Science B.V. All rights reserved.

Keywords: Ceria–terbia; Ceria; Platinum; Oxygen buffering; Oxygen storage; CO oxidation; CH$_4$ oxidation

1. Introduction

Ceria has been widely used for TWC applications because of its remarkable redox properties. The capacity of ceria to store and release oxygen enables the car-exhaust purification catalyst to operate more efficiently by making it less sensitive to the continuous lean/rich oscillations occurring in the exhaust stream [1]. However, the performance of the ceria-based three-way catalysts during the so-called ‘cold start period’ of engines must be improved to meet the increasingly restrictive regulations on exhaust emissions from automobiles. In particular, new materials with enhanced oxygen storage (OSC) and oxygen buffering (OBC) capacities are demanded [2].

Earlier studies [3,4] have shown the outstanding redox properties of a ceria–terbia mixed oxide with reference to those exhibited by pure ceria and pure terbia. The temperature window in which the mixed oxide is effective considerably widens that exhibited by pure oxides, with a maximum oxygen release at lower temperature than that determined for the other single oxides.

Herein, we report on the redox behaviour and catalytic properties of a 1% Pt/CeTbO$_x$ catalyst. By using a combination of OSC, OBC, and catalytic conversion measurements for both methane and carbon monoxide oxidation reactions, the properties of this catalyst are outlined in comparison to those exhibited by a classic Pt/CeO$_2$ catalyst of similar characteristic used as reference. The whole ensemble of results presented here bring us to conclude that the incorporation to ceria of a second reducible rare earth cation like terbium should be considered in the future for the rational design of the new generation of TWC materials.

---

* Corresponding author.

PII: S0920-5861(99)00148-0

2. Experimental

The Ce–Tb mixed oxide employed as support of platinum in the present work was prepared by co-precipitation from an aqueous solution of the corresponding nitrates, after addition of concentrated ammonium hydroxide. For this purpose, 25 g of $Tb(NO_3)_3 \cdot 5\,H_2O$ and 100 g of $Ce(NO_3)_3 \cdot 6\,H_2O$, both 99.99% pure from Aldrich, were dissolved separately in distilled water (100 and 300 ml, respectively) and the resulting solutions, mixed together. Fifty millilitres of a 25% ammonia solution, from Merck, were slowly added to the nitrate mixture and the solid so obtained washed, filtered and dried in oven during 12 h at 130°C. After milling and grinding the dried product, a final calcination step at 600°C was applied in order to decompose the mixed oxide precursor. Specifically, a treatment in air at high temperature, 900°C, was selected in order to get a Ce–Tb mixed oxide with stable surface area. By doing this, metal particle encapsulation processes associated to further high temperature reduction treatments can be minimised.

Using the procedure described above, a homogeneous $Ce_{0.8}Tb_{0.2}O_{2-x}$ mixed oxide, hereafter referred to as $CeTbO_x$, with $8\,m^2\,g^{-1}$ surface area and without microporosity was prepared. The nominal chemical composition of this oxide was confirmed by ICP analysis of a series of previously dissolved oxide samples [5]. Further characterisation details about this oxide can be found in Ref. [3]. Cerium dioxide with a surface area of $4\,m^2\,g^{-1}$ was used as support of the catalyst used as reference. Both the Ce/Tb mixed oxide and the pure CeO_2 sample appeared by XRD and HREM to be fluorite-like homogeneous materials. Starting from these oxides, 1 wt% Pt catalysts were prepared by incipient impregnation with an aqueous solution of $[Pt(NH_3)_4](OH)_2$. After impregnation, the catalysts were dried in oven at 110°C for 12 h. Prior to any measurement, the samples were always pre-treated in a flow of O_2(5%)/He at 500°C for 1 h, cooled slowly to 100°C under the oxidising mixture, and then to room temperature in pure He. This standard pre-treatment guarantees a common well-defined starting redox state throughout our whole study.

The reduction treatments applied to the catalyst precursors were done in a flow of H_2(5%)/Ar (60 ml min^{-1}) at a heating rate of 10°C min^{-1}. The catalysts were held for 1 h at the selected reduction temperature and further evacuated at the reduction temperature for 1 h under flowing He. In the case of the OSC experiments, a reduction time of 1 min was selected.

Prior to the OBC runs, the samples were reduced following the general reduction treatment described above. After reduction, the gas flow was turned to He and the temperature set to the value selected for carrying out the test. The experimental method for OBC measurements has been already described in Ref. [4](3). Briefly, it consists of injecting 0.25 ml O_2(5%)–He pulses, at 10 s intervals, in the 60 ml min^{-1} inert gas stream. The oscillations monitored with a thermal conductivity detector at the outlet of the reactor are the result of the balance of the oxygen injected, consumed and released by the catalyst. Thus, the efficiency of a sample as an oxygen buffer can be accounted by the attenuation factor, defined as the ratio of the steady-state amplitude of the oscillations in the absence of sample to the amplitude in its presence [4].

The OSC experiments were performed with a VG Sensorlab 200D Mass Spectrometer as analytical device. The samples were reduced at a given temperature in flowing H_2(5%)/Ar for 1 min, and then treated at the same temperature with pure Ar (30 ml min^{-1}) before cooling to 150°C. At this temperature, pulses of 0.5 ml of O_2 (5%)/He were injected periodically at intervals of 2 min and the oxygen uptake monitored.

The ‘light-off’ curves for methane and carbon monoxide oxidation were recorded in a flow U-shaped reactor. The amount of oxide catalyst was always 100 mg. The stoichiometric reaction mixture was prepared with the help of mass flow controllers; it consisted of 20 ml min^{-1} CH_4(5%)/He and 40 ml min^{-1} of O_2(5%)/He, in the case of methane oxidation, and 60 ml min^{-1} CO(5%)/He and 30 ml min^{-1} of O_2(5%)/He in the case of carbon monoxide oxidation. The space velocities were 50 000 and 86 000 h^{-1}, respectively.

3. Results and discussion

Fig. 1 shows a representative image of the $Pt/CeTbO_x$ catalyst reduced at 350°C. Fringe pattern analysis of this image by digital Fourier Transform

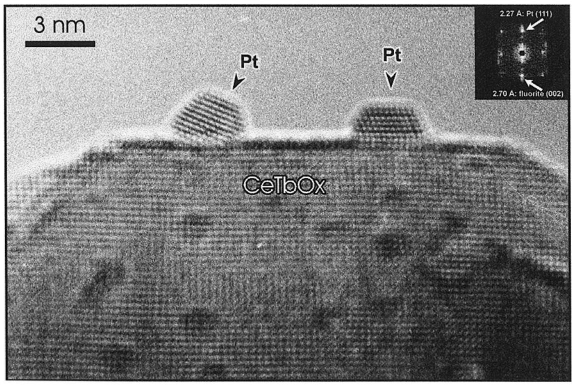

Fig. 1. HREM image representative of the Pt/CeTbO$_x$ catalyst reduced at 350°C. Inset corresponds to the digital diffractogram obtained on the supported particles.

techniques allows us to detect the presence of platinum particles, as indicated in Fig. 1. In effect, the 0.23 nm lattice spacing measured on the particles seen on the surface of the mixed oxide crystallites can be assigned to the (1 1 1) planes of Pt (0.227 nm). This assignment can be also confirmed by using HREM image simulation [6].

Another remarkable detail in Fig. 1 is that the surfaces of the metal particles look like flat and clean. By measuring on different HREM micrographs the diameter of several hundreds of metal microcrystals, the size distribution and metal dispersion of platinum for this sample could be established. As it can be observed in Fig. 2(a), the main core of the distribution corresponding to the catalyst reduced at 350°C is rather narrow, with 90% of the metal particles showing sizes below 3.5 nm. From this histogram, a mean particle diameter of 2.5 nm could be established. The average particle size on the Pt/CeO$_2$ catalyst was estimated to be 2.8 nm.

Fig. 2(b) accounts for the contribution to the metal dispersion of the particles with a predefined d_k value or smaller, as a function of d_k. As described in further detail in Ref. [7], the accumulated dispersion can be calculated as:

$$\frac{[\Sigma_i N_i(\mathrm{Pt_s})(d_i \leq d_k)]}{N_\mathrm{t}(\mathrm{Pt})}$$

where $N_i(\mathrm{Pt_s})$ is the number of surface platinum atoms in particles with size d_i and $N_t(\mathrm{Pt})$ the total number of platinum atoms. These values were calculated by using the equations developed by Van Hardeveld and Hartog [8]. In accordance with Ref. [7], a cubo-octahedron-truncated morphology was assumed for platinum particles.

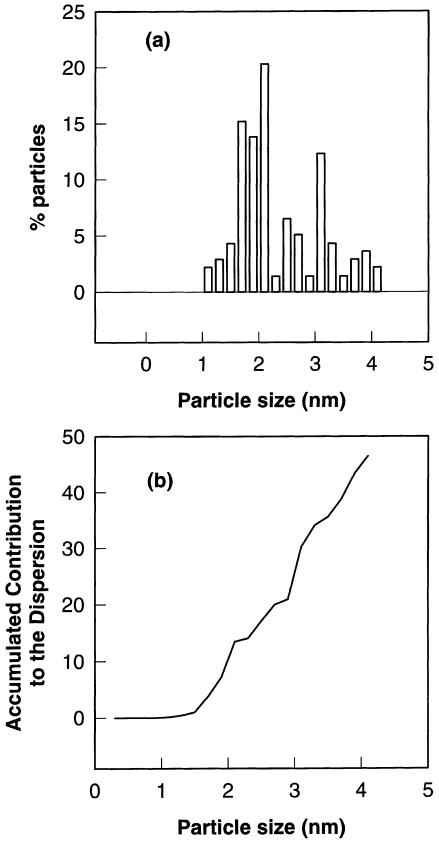

Fig. 2. Particle size distribution (a) and accumulated dispersion as a function of the particle size (b) established from the HREM images for the Pt/CeTbO$_x$ catalyst reduced at 350 °C.

The last point of the whole distribution curve in Fig. 2(b) measures the metal dispersion of the catalyst: 45%.

The metal particle dispersion did not change after reduction at 500°C, thus proving that no sinterization process occurs when this sample is treated under reducing conditions within the temperature range 350–500°C.

Fig. 3 shows the TC signals for OBC experiments carried out at 500°C on Pt/CeO$_2$ (a) and Pt/CeTbO$_x$ (b) catalysts. The oscillations in Fig. 3(a) are coincident with those obtained in a blank test without

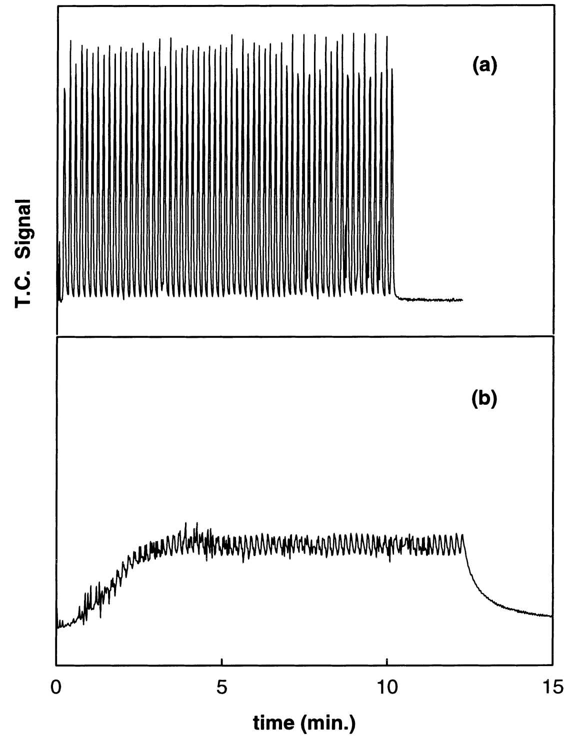

Fig. 3. TC signals for OBC experiments at 500°C on Pt/CeO$_2$ (a) and Pt/CeTbO$_x$ (b) catalysts.

sample, thus indicating that Pt/CeO$_2$ does not have any oxygen buffering capacity at the selected temperature and operation conditions.

In the case of the Pt/CeTbO$_x$ catalyst, Fig. 3(b) clearly shows how this catalyst attenuates the oscillations of the oxygen partial pressure induced by the pulses. Initially, the pulses are partially consumed by the catalyst, thus gradually increasing its oxidation level. After the first 2 min, the catalyst reaches a steady state in which its oxygen buffering ability is extremely high. When the injections cease after 12 min, the sample gradually returns to its initial equilibrium state in the flowing He carrier. The excellent behaviour of the Pt/CeTbO$_x$ catalyst relates to the ability of the mixed oxide to rapidly change its composition in response to the pulses. It is through these changes, favoured by the presence of metal dispersed, that the catalyst can attenuate the oxygen pressure oscillations. It undergoes oxidation when the atmosphere is rich in oxygen and reduction when the oxygen partial pressure in the flowing gas is low.

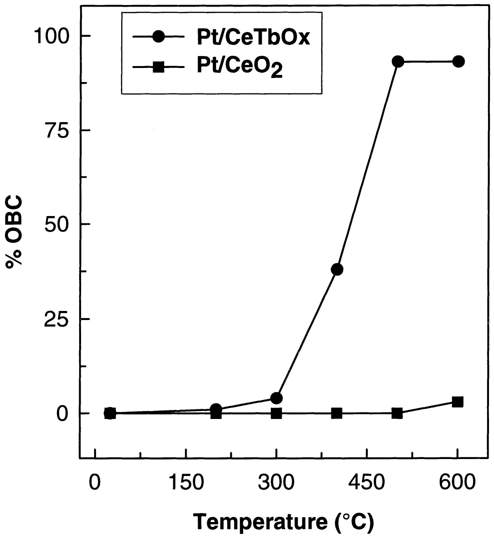

Fig. 4. Attenuation factors from OBC experiments as a function of the temperature for Pt/CeTbO$_x$ and Pt/CeO$_2$ catalysts.

The quantitative results for OBC experiments at different temperatures are reported in Fig. 4. The attenuation factor of the Pt/CeTbO$_x$ sample is close to 100% at 500°C. This clearly contrasts with the Pt/CeO$_2$ reference, which does not show any measurable buffer capacity below 600°C. Also worth noting, as deduced from Fig. 4., the difference in oxygen buffering capacity for the two catalyst is already significant at 350°C. This behaviour of the catalyst is highly remarkable, suggesting very interesting properties as oxygen buffer material in a domain of temperatures relevant for TWC applications.

The very interesting redox properties of the Pt/CeTbO$_x$ catalyst are confirmed by the OSC data shown in Fig. 5.

In accordance to some earlier studies [3], CeTbO$_x$ mixed oxides are able to release oxygen when treated under oxidising conditions at temperatures above 200°C. This fact brought us to measure the oxygen uptake by pulsing at 150°C, this temperature being the maximum temperature at which only consumption and, therefore, no simultaneous production of oxygen occurs. The oxygen storage capacity observed in the case of Pt/CeO$_2$ catalyst after a very short (1 min) reduction treatment was negligible at temperatures below 700°C.

The oxygen uptake for our Pt/CeTbO$_x$ catalyst was 88 μmol per gram of catalyst after reduction at 350°C,

Table 1
Light-off temperatures (°C) of Pt/CeTbO$_x$ and Pt/CeO$_2$ catalysts

CH_4 Oxidation[a]			CO Oxidation[b]		
Reduction temperature (°C)	Pt/CeTbO$_x$	Pt/CeO$_2$	Reduction temperature (°C)	Pt/CeTbO$_x$	Pt/CeO$_2$
200	317	553	200	118	151
500	317	523	500	117	153

[a] Flow: 20 ml min^{-1} CH_4 (5%)/He + 40 ml min^{-1} O_2(5%)/He.
[b] Flow: 60 ml min^{-1} CO (5%)/He + 30 ml min^{-1} O_2(5%)/He.

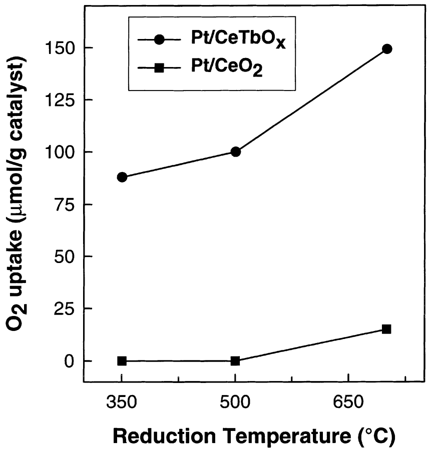

Fig. 5. Oxygen uptake at 150°C as a function of the reduction temperature for Pt/CeTbO$_x$ and Pt/CeO$_2$ catalysts.

this OSC increasing as the temperature of reduction rises, as showed in Fig. 5.

Considering that only a 45% of the platinum atoms are exposed, and supposing that only platinum sited on the particles surface are oxidised, the fraction of oxygen uptake corresponding to oxidation of the metal can be estimated. It has been found to be 8 μmol of O_2 per gram of catalyst, which represents less than a 10% of the lower value found for the OSC of the Pt/CeTbO$_x$ catalyst. Also worth of noting, the amount of oxygen stored by the Pt/CeTbO$_x$ catalyst reduced at 350°C is ~4 times larger than that estimated for a purely surface reduction from the BET surface area for this sample (8 m^2 g^{-1}). Therefore, oxygen from the bulk of the particles must participate in the exchange process and contribute to the oxygen storage. Reduction treatments at higher temperatures lead to an increase in the oxygen uptake, as commented above, making the contribution of the bulk oxygen much more evident.

In accordance with Ref. [3], the results from OBC and OSC measurements showed here strongly suggest that the incorporation of terbium cations into the fluorite-like structure of ceria promotes its reduction at moderate temperatures through the creation of oxygen vacancies. The presence of vacancies, probably associated to Tb^{3+} ions [9], could enhance the bulk oxygen mobility, thus increasing the capacity of the mixed oxide to store oxygen and its ability to rapidly reach the equilibrium composition determined by both the temperature and the oxygen partial pressure, this being considered as a key property for buffering materials.

Finally, Table 1 shows some data regarding the catalytic essays. It has been demonstrated that ceria promotes precious-metal catalysts for both the CO and CH_4 oxidation reactions [10,11]. It can be seen in Table 1 that the ‘light-off’ temperatures associated to 50% conversion of CO on the Pt/CeTbO$_x$ catalyst are much lower than the values obtained for Pt/CeO$_2$. The same trend was observed when total oxidation of methane was investigated. In both cases, the light-off temperatures of CO and CH_4 oxidation reactions do not change with the reduction temperature. These results are in good agreement with those reported above and give us an additional indication of the improvement of performance achieved in the CeTbO$_x$-supported platinum catalyst.

4. Conclusions

The properties of a Pt/CeTbO$_x$ catalyst have been investigated and compared to those exhibited by a classic Pt/CeO$_2$ model system.

It has been shown that the modification of pure ceria by addition of 20 mol% of terbia significantly increases not only the capability of Pt/CeO_2 catalysts to store oxygen but also its ability to attenuate the oscillations of the oxygen partial pressure.

The ensemble of these observations and the values found for the ‘light-off’ temperatures for methane and carbon monoxide oxidation allow us to conclude that the $CeTbO_x$ mixed oxide may be considered as an interesting alternative material for advanced TWC applications. In particular, the OBC and OSC results point to its excellent redox response under the so-called ‘cold start’ operation conditions.

Acknowledgements

This work has received financial support from the CICYT (Project MAT96-0931), the DGICYT (Project PB95-1257) and the Junta de Andalucía. The HREM image reported in this work was obtained at the Electron Microscopy Facilities of the University of Cádiz.

References

[1] K.C. Taylor, Proc. First International Symposium on Catalysis and Automotive Pollution Control, Brussels, 8–11 September 1986.

[2] P. Degobert, Automobiles and Pollution, Society of Automotive Engineers, Inc., 1995.

[3] S. Bernal, G. Blanco, M.A. Cauqui, P. Corchado, J.M. Pintado, J.M. Rodriguez-Izquierdo, Fourth International Symposium on Catalysis and Automotive Pollution Control (CAPOC-4), Brussels, 9–11 April 1997.

[4] S. Bernal, G. Blanco, M.A. Cauqui, P. Corchado, J.M. Pintado, J.M. Rodriguez-Izquierdo, Chem. Commun, 1997, 1545–1546.

[5] G. Blanco, Ph.D. Thesis, University of Cádiz, Cádiz, 1997.

[6] S. Bernal, G. Blanco, J.J. Calvino, M.A. Cauqui, P. Corchado, C. López-Cartes, J.A. Pérez-Omil, unpublished results.

[7] S. Bernal, J.J. Calvino, M.A. Cauqui, J.A. Pérez-Omil, J.M. Pintado, J.M. Rodriguez-Izquierdo, Appl. Catalysis B: Environmental 16 (1998) 127.

[8] R. Van Hardeveld, F. Hartog, Surf. Sci., 15 (1969) 189, preprint.

[9] M.Y. Sinev, G.W. Graham, L.P. Haack, M. Shelef, 11th International Congress on Catalysis, Baltimore, 1996, Po-12.

[10] H. Cordatos, R.J. Gorte, J. Catal. 139 (1996) 112.

[11] M. Haneda, T. Mizushima, N. Kakuta, J. Chem. Soc. Faraday Trans. 91(24) (1995) 4459.